

Received: 2018.04.21

Accepted: 2018.06.28

Published: 2018.11.07

Protective Effect of Anthocyanin on Paraquat-Induced Apoptosis and Epithelial-Mesenchymal Transition in Alveolar Type II Cells

Authors' Contribution:

Study Design A

Data Collection B

Statistical Analysis C

Data Interpretation D

Manuscript Preparation E

Literature Search F

Funds Collection G

AB Zhihua Wang

BC Dongming Gu

DE Lezhi Sheng

FG Jinfang Cai

Emergency Department of Traumatology, Shanghai Pudong Hospital, Shanghai, P.R. China

Corresponding Author: Jinfang Cai, e-mail: caijinfang_jfc@163.com

Source of support: This work was funded by Key Discipline Construction Project of Pudong Health Bureau of Shanghai (Grant NO.PWZxk2017-20)

Background: Paraquat (PQ) can over-accumulate in alveolar epithelial cells. Anthocyanin (An) can exert anti-oxidative properties. The role of An in PQ-induced toxicity is unclear, so we aimed to explore whether An could inhibit epithelial mesenchymal transition (EMT) induced by PQ in alveolar cells.


Material/Methods: Alveolar epithelial cells were treated with PQ and An with concentration gradient for 12, 24, and 48 h. The cell viability, ROS level, and apoptosis rate were determined using the Cell Counting Kit-8 (CCK-8) and flow cytometry, respectively. The lactate dehydrogenase (LDH) leakage, methane dicarboxylic aldehyde (MDA) level, glutathione peroxidase (GPx), and superoxide dismutase (SOD) activities were determined by spectrophotometric method. The mRNA and protein expressions were detected using quantitative real-time PCR (qPCR) and Western blot, respectively.

Results: An reduced the PQ-induced apoptosis in a dose-dependent manner. Moreover, An reduced the ratio of Bax/Bcl-2 to ROS level. We found that An suppressed the activity of LDH and MDA and improved SOD and GPX levels. Additionally, the level of PQ-induced E-cadherin was decreased by An while the expressions of vimentin, α -smooth muscle actin (α -SMA), and collagens type I (col-I) were increased. Furthermore, An inhibited the levels of transforming growth factor β 1 (TGF- β 1) and activin receptor-like kinase 5 (ALK5) and reduced the phosphorylation of smad2.

Conclusions: Our study shows newly discovered effects of anthocyanidins on EMT and supports their chemopreventive effects in paraquat-induced apoptosis in alveolar type II cells.

MeSH Keywords: **Anthocyanins • Apoptosis • Epithelial-Mesenchymal Transition • Paraquat**

Full-text PDF: <https://www.medscimonit.com/abstract/index/idArt/910730>

 1986

 1

 5

 46



Background

Paraquat (PQ, 1, 1'-dimethyl-4, 4'-bipyridinium) can accumulate to an especially high level in alveolar type II (AT2) epithelial cells; it is an extremely poisonous substance and its primary pathological target organ is the lungs [1–3]. PQ-induced acute pulmonary fibrosis can cause respiratory failure, thus leading to death [4,5]. Lung epithelial cells can acquire mesenchymal properties by epithelial-mesenchymal transition (EMT), which is expressed as decreased epithelial cell markers (E-cadherin) and increased mesenchymal cell markers (vimentin) [6]. Epithelial cells can be transformed to mesenchymal cells during the EMT process [7]. Moreover, EMT was revealed to be involved in lung fibrosis [8,9].

It was reported that PQ can cause fatal human toxicity by an oxidation-reduction cycle, as well as accumulating reactive oxygen species [10,11], which contributes to oxidative damage to cells. Apoptosis of alveolar epithelial cells is regarded as another molecular mechanism of PQ-induced lung injury [12–14]. Several drugs were reported to be effective against PQ toxicity, but they exert little effect in PQ-induced lung injury.

Recently, many studies have demonstrated that PQ-induced lung toxicity can be alleviated primarily by antioxidant [15–18] and anti-apoptotic [13,19] pathways. Anthocyanins (An) have been reported to protect against cellular oxidation and inhibit oxidant-induced inflammatory cell damage and cytotoxicity [20–25]. Recently, An was shown to suppress the TGF- β /smad2 signaling pathway via inhibition of EMT in glioblastoma cells [26]. However, the effect of anthocyanin on PQ-induced apoptosis and EMT is still unclear. Therefore, the present study was performed to explore the potential mechanism of anthocyanin in PQ-induced lung injury.

Material and Methods

Reagents

Anthocyanins were obtained from Extrasynthese (Genay, France). RPMI-1640 media, fetal bovine serum (FBS), and paraquat solution were purchased from Sigma-Aldrich (St. Louis, MO, USA). RIPA, Cell Counting Kit-8 (CCK-8), 2', 7'-dichlorofluorescein diacetate (DCFH-DA), sodium dodecyl sulfate polyacrylamide gel electrophoresis (SDS-PAGE), and BCA protein assay kits were purchased from Beyotime Institute of Biotechnology (Haimen, Jiangsu, China). Kits used for lactate dehydrogenase (LDH), methane dicarboxylic aldehyde (MDA), glutathione peroxidase (GPx), and superoxide dismutase (SOD) detection were purchased from the Jiancheng Institute of Bioengineering (Nanjing, China). Trizol was purchased from Invitrogen (Carlsbad, CA) and the FastQuant RT Kit was purchased from TIANGEN

(Beijing, China). Antibodies used for Western blot analyses were anti-Bcl-2, anti-Bax, anti-vimentin, anti-TGF- β 1, anti-ALK5, and anti- β -actin (Santa Cruz Biotechnology, Santa Cruz, CA, USA); anti-phospho-smad2 (p-smad2) and anti-smad2 (Cell Signaling Technology, Beverly, MA); anti-E-cadherin, anti- α -SMA, and anti-col-I (Abcam, Cambridge, MA, USA); and horseradish peroxidase (HRP)-conjugated antibody (Sigma-Aldrich, St. Louis, MO, USA).

Cell culture and treatment

RLE-6TN cells were purchased from the American Type Culture Collection (ATCC; Manassas, VA, USA). RLE-6TN cells were maintained in RPMI-1640 media containing 10% FBS at 37°C with 5% CO₂ in an incubator. For CCK-8, cells were incubated with concentration gradient of PQ (0, 5, 25, 50, and 100 μ M) and An (0, 10, 20, 40, and 80 μ M) for 12, 24, and 48 h, respectively. Moreover, cells were treated by PQ with different levels of An (20, 40, and 80 μ mol/L) for 12, 24, and 48 h.

CCK-8 assay

Cells (1×10^4) were cultivated and then CCK-8 was added to each group for 4 h. Absorbance was measured at 450 nm using a MultiSkan3 ELISA Reader (Thermo Fisher scientific, USA).

Detection of cell apoptosis

Cell apoptosis in each group was analyzed by Annexin V-PE apoptosis detection kit according to the manufacturer's protocol (BD Biosciences, San Jose, CA, USA). Cell apoptosis was analyzed by flow cytometry (Guava Technologies, Inc., Millipore, USA). Data analysis was performed using FCS ExpressV3 software (De Novo Software, Los Angeles, CA). Cells in each group were identified by fluorescent staining: Annexin V-PE stained cells represented early apoptotic cells, 7-AAD bounded cells represented necrotic cells, and double-labeled cells represented late apoptotic cells.

ROS determination

The cells (2×10^5) were cultivated in a 6-well plate. Thereafter, DCFH-DA (10 mM) was added in the medium and incubated in the dark at 37°C for 0.5 h. The cells were measured by flow cytometry (Guava Technologies, Inc., Millipore, USA).

Measurement of LDH, MDA, SOD, and GPx activity

The cells were incubated and centrifuged for the measurement of LDH leakage, MDA level, SOD, and GPx activities. The content of LDH release, MDA level, and SOD activities were determined according to the manufacturer's protocol. The absorbance was read using a Hitachi U-2000 recording spectrophotometer (Tokyo, Japan).

Table 1. Primers for qPCR.

Gene	Forward primers (5'-3')	Reverse primers (5'-3')
E-cadherin	GGGTTGTCTCAGCCAATGTT	CACCAACACACCCAGCATAG
α-SMA	AGCCAGTCGCCATCAGGAAC	CCGAGGCCATTGTACACACAC
Vimentin	AGATCGATGTGGACGTTTCC	CACCTGTCTCCGGTATTCTGT
Col-1	TGCTGCCTTTTCTGTTCTT	AAGGTGCTGGGTAGGGAAGT
Bax	GCCTTTTGTACAGGGTTTCA	CACAAAGATGGTCACTGTCTGC
Bcl-2	ATAAGCTGTACAGAGGGGCTA	CGGTTCAAGTACTCAGTCATCC
β-actin	TTGCCGATAGTGATGACCT	CGTGCGTGACATTAAGAG

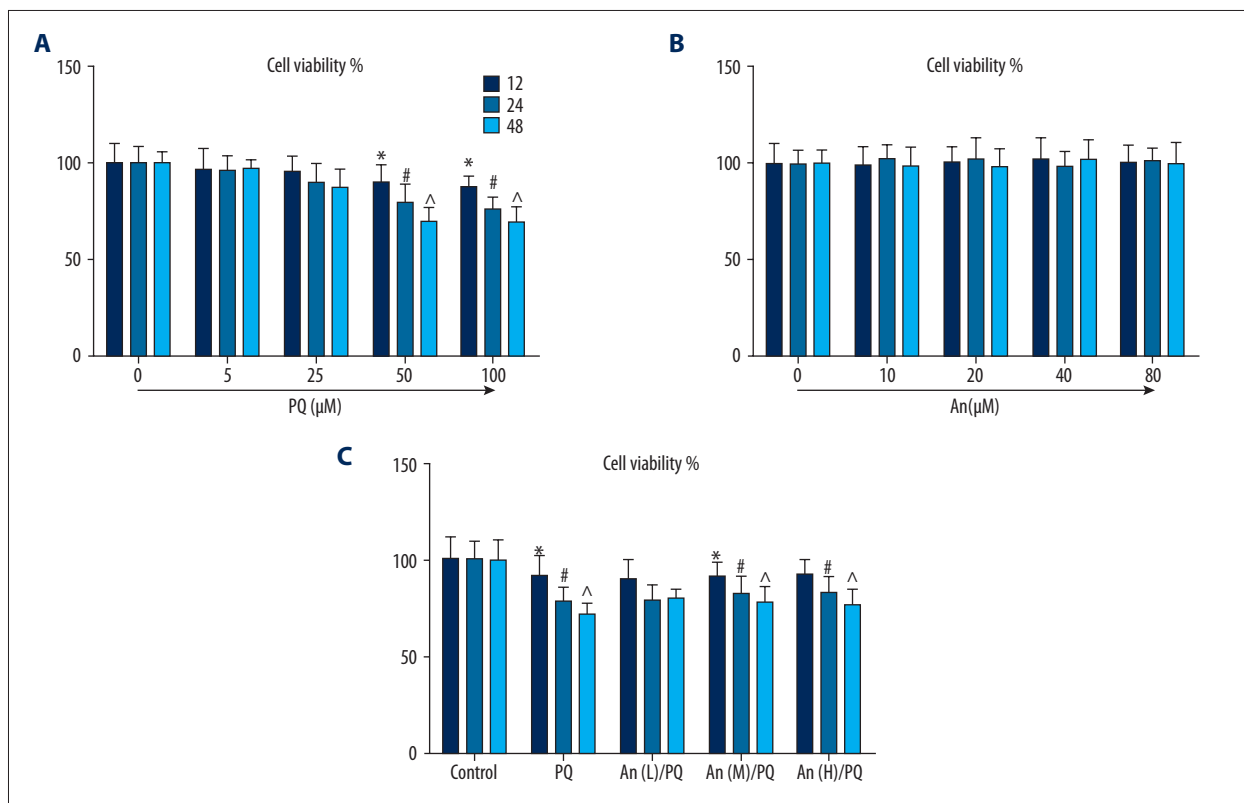


Figure 1. An increased the viabilities of RLE-6TN cells treated by PQ. (A) The cell viabilities of the RLE-6TN cells decreased with the increased concentration of PQ administered for 12, 24, and 48 h. (B) The viability of RLE-6TN cells was maintained by different doses of An for 12, 24, and 48 h. (C) The viability of RLE-6TN cells treated by PQ (50 μM) were increased by low (20 μM), medium (40 μM), and high (80 μM) concentrations of An. *, #, ^ P<0.05 compared with control group.

Quantitative real-time polymerase chain reaction (qRT-PCR)

Total RNA of cells (5×10⁵) in each group was extracted by Trizol reagent and the concentrations and the purity were determined. Then, cDNA was reversed according to the kit protocol. The qPCR reactions were performed in the ABI 7900 PCR system (Applied Biosystems, Foster City, CA, USA) with the following conditions: 95°C for 10 min, 40 cycles of 95°C for 15 s, and 60°C for 1 min. The specific primers are shown in Table 1. GAPDH

served as a reference gene and each sample were detected at least 3 times. The results were evaluated by 2^{-ΔΔCT} method.

Western blotting

RLE-6TN cells were lysed in lysis buffer followed by the determination of protein concentrations by a BCA kit. Total proteins severed by SDS-PAGE were transferred onto polyvinylidene difluoride membranes (GE Healthcare, Little Chalfont, United Kingdom). The membranes were incubated overnight

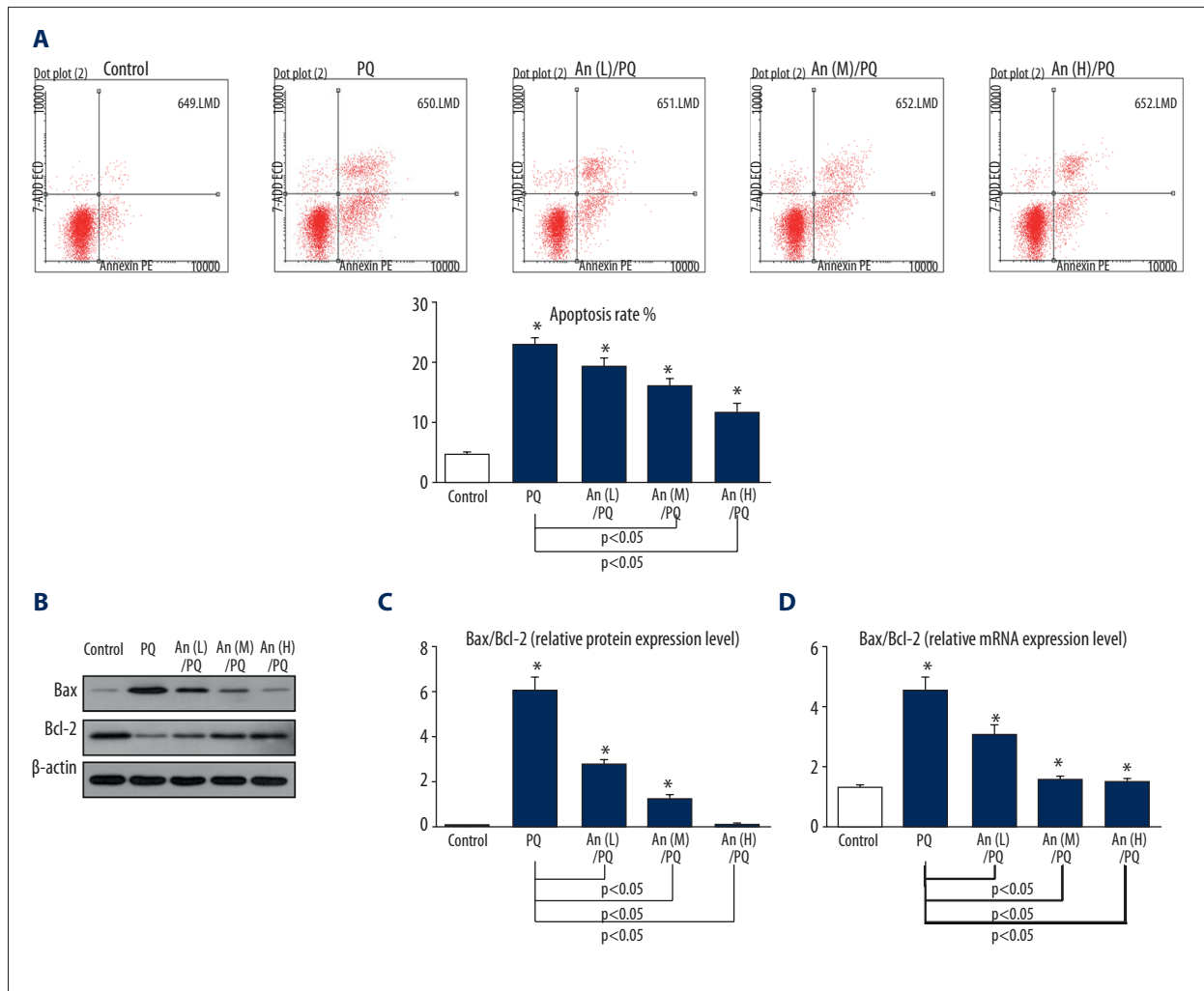


Figure 2. An inhibited the PQ-induced apoptosis of RLE-6TN cells. **(A)** The apoptosis rate in each group as shown by flow cytometry. **(B–D)** Western blot and qPCR results showed that the ratios of Bax/Bcl-2 were decreased by An. * $P < 0.05$ compared with control group.

at 4°C with primary antibodies after blocking with 5% nonfat milk solution. The membranes were washed and finally incubated with HRP-conjugated secondary antibodies (1: 3000). The proteins were detected using the Molecular Imager VersaDoc MP 5000 System (Bio-Rad Life Science Research, Hercules, CA) and analyzed with Quantity One software v4.6.9 (Bio-Rad, Hercules, CA).

Statistical analysis

Data are expressed as the mean \pm SEM. One-way analysis of variance (ANOVA) was used to evaluate the differences among groups. A value of $P < 0.05$ was considered statistically significant. All statistical analyses were performed using SPSS software (version 15.0, SPSS, Chicago, IL, USA).

Results

An improved the decreased cell viability induced by PQ

PQ reduced the cell viability in a dose-dependent manner, and 50 μ M PQ significantly inhibited the cell viability (Figure 1A). An had very little effect on the proliferation of normal RLE-6TN cells (Figure 1B). However, 24 or 48 h after An treatment, the decreased cell viability caused by PQ was obviously increased by An (Figure 1C).

An inhibited the PQ-induced apoptosis in a time- and dose-dependent manner

When the cells were exposed to PQ, the total number of apoptotic cells was increased by more than 20%, while An inhibited cell apoptosis in a dose-dependent manner (Figure 2A).

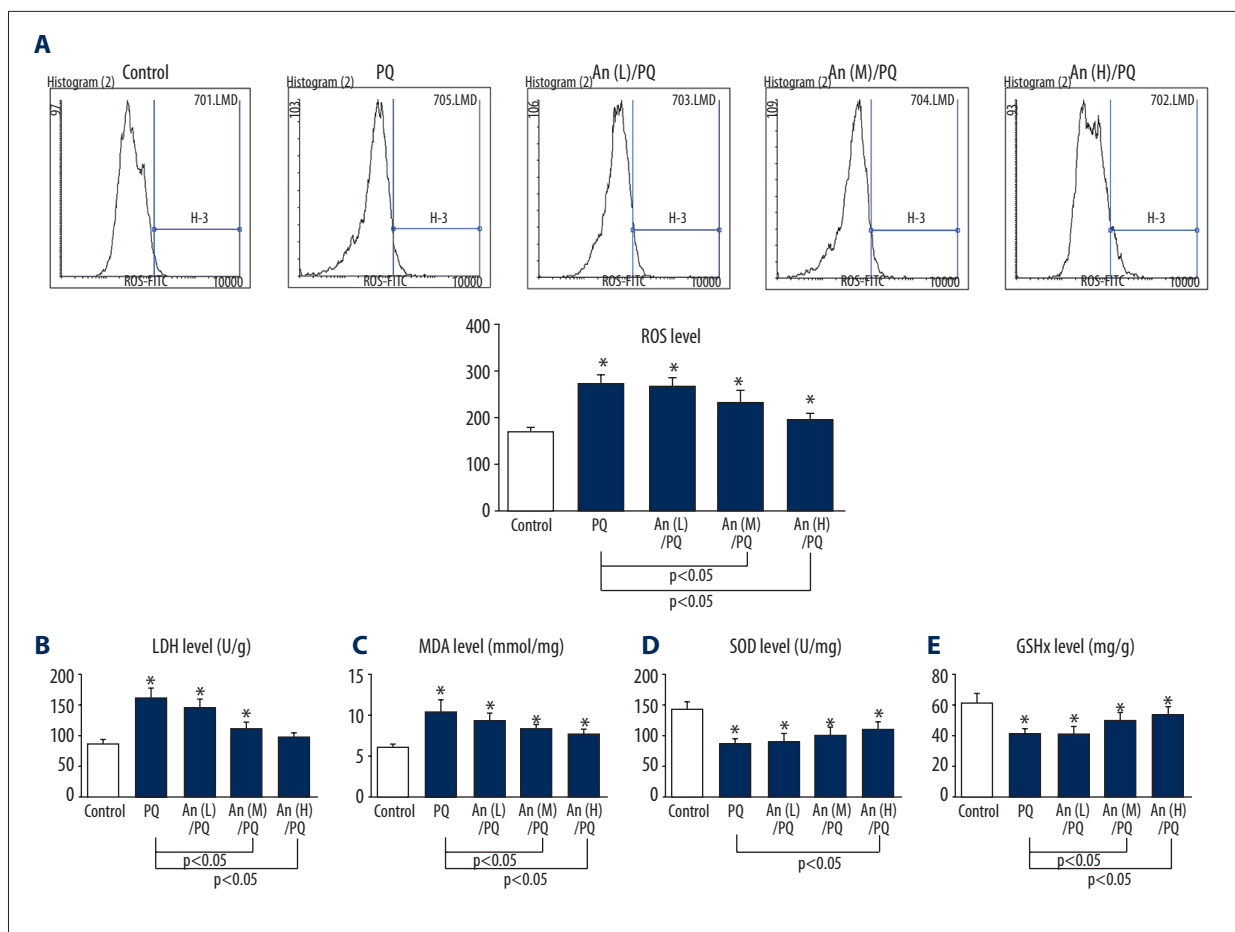


Figure 3. An attenuates the PQ-induced oxidative stress in RLE-6TN cells. (A) The ROS level in each group was detected by flow cytometry. The levels of (B) LDH, (C) MDA, (D) SOD, and (E) GPx were measured by commercial kits. * $P < 0.05$ compared with control group.

Furthermore, Western blot results showed that An suppressed the level of Bax but enhanced the expression of Bcl-2 (Figure 2B). The ratios of Bax/Bcl-2 were also decreased by An at protein and mRNA levels (Figure 2C, 2D).

An attenuated PQ-induced oxidative stress in RLE-6TN cells

The ROS level was evidently increased by PQ, and low concentration of An could not inhibit the ROS level. Moreover, the high level of An significantly reduced ROS accumulation (Figure 3A). Additionally, a remarkable increase in LDH leakage was observed in cells treated by PQ compared with the control group. However, the increased LDH release was reduced by An (Figure 3B). Similarly, the obviously increased levels of MDA induced by PQ were reduced by An (Figure 3C). Additionally, the activities of SOD and GPx in the PQ group were obviously decreased compared with the control group, whereas the high level of An partly recovered the decreased levels of SOD and GPx (Figure 3D, 3E).

An regulated the EMT-related molecules in RLE-6TN cells

The expression of E-cadherin was obviously decreased by PQ, while the levels of α -SMA, vimentin, and col-1 were increased by PQ treatment. However, An reversed the expression patterns. Moreover, the expressions of PQ-induced α -SMA and vimentin were largely suppressed to the control levels by the high level of An (Figure 4A–4D). Western blot results showed a similar protein expression trend as with mRNA (Figure 4E). An improved the protein expression and suppressed the protein levels of α -SMA, vimentin, and col-1 (Figure 4F–4I).

An suppressed the levels of TGF- β 1 and ALK5 as well as the phosphorylation of smad2 in RLE-6TN cells

To further illuminate the potential mechanism of An in PQ-induced EMT, the protein levels of TGF- β 1, ALK5, p-smad2, and smad2 were determined in RLE-6TN cells (Figure 5A). The levels of PQ-induced TGF- β 1 (Figure 5B) and ALK5 (Figure 5C)

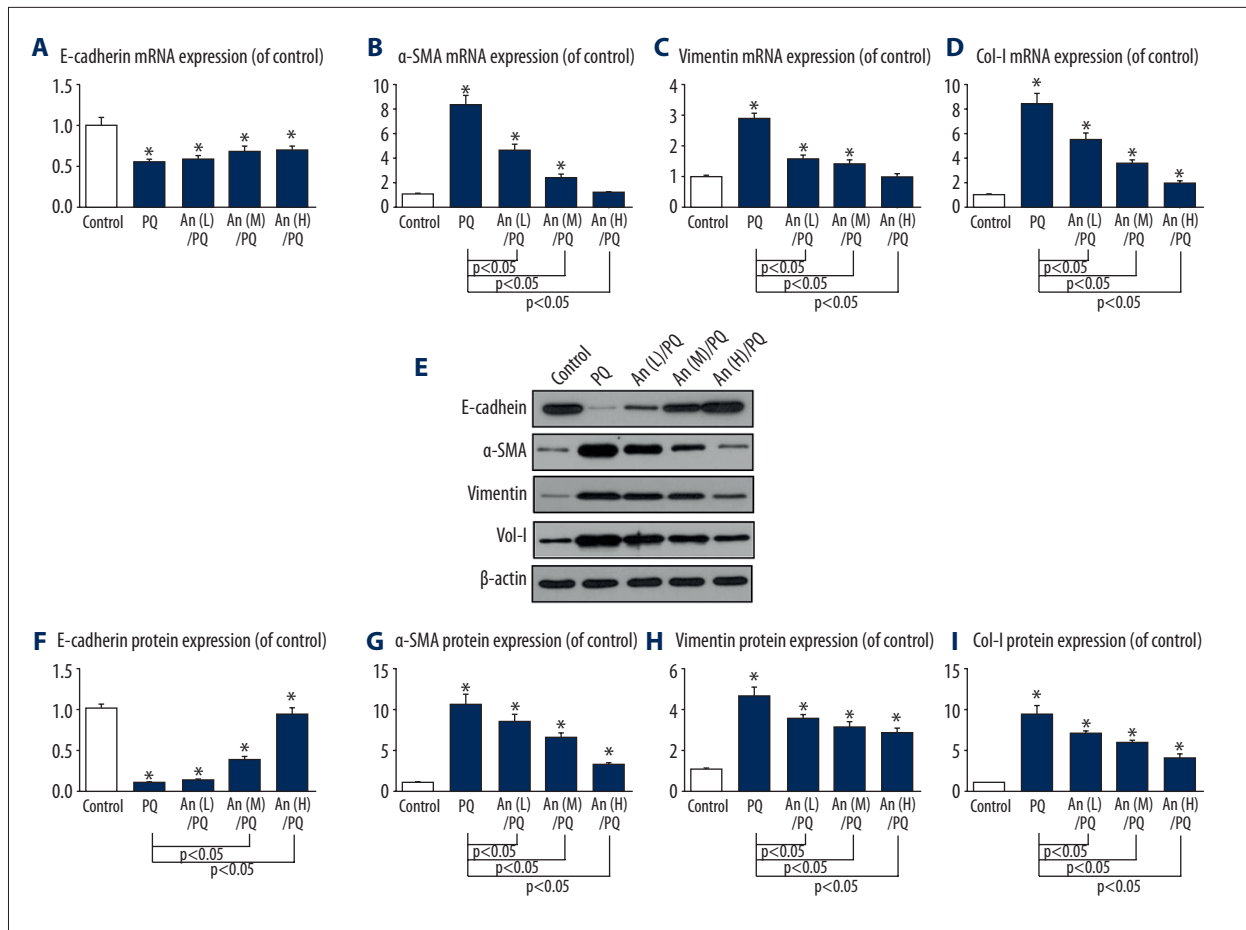


Figure 4. An regulated the EMT-related molecules in RLE-6TN cells. The mRNA levels of (A) E-cadherin, (B) α-SMA, (C) vimentin, and (D) col-I were determined by qPCR. (E-I) The protein levels of E-cadherin, α-SMA, vimentin, and col-I by as indicated by Western blot analysis. * $P < 0.05$ compared with control group.

were significantly reduced by An. Furthermore, the ratio of p-smad2/smad2 was markedly decreased by An (Figure 5D).

Discussion

Oxidative stress, inflammation, and pneumocyte apoptosis may play roles in the pathology of PQ-induced pulmonary fibrosis [27–30]. In the present study, the major finding was that An attenuated the PQ-induced apoptosis and regulated the EMT-related molecules in RLE-6TN cells. Furthermore, An not only inhibited the levels of TGF-β1 and ALK5, but also the phosphorylation of smad2 in the RLE-6TN cells.

According to several *in vitro* experiments, PQ caused apoptosis of various cells [12,31,32]. In our study, the high concentration of PQ led to the apoptosis of RLE-6TN cells, confirming that acute PQ injury can trigger apoptosis, in line with results of a previous study [6]. An improved the viability of PQ-treated RLE-6TN cells in time- and dose-dependent manners. Moreover, the

apoptosis rate induced by PQ was significantly suppressed by An. Furthermore, the pro- and anti-apoptosis members of the Bcl-2 family were reported to serve as an index for cell apoptosis [33]. An inhibited the expression of Bax (pro-apoptosis) and up-regulated the Bcl-2 (anti-apoptosis) level, indicating that An can attenuate PQ-induced cytotoxicity and apoptosis.

ROS have been reported to play a critical role in PQ-induced lung toxicity [29]. In the present study, high-dose An almost reduce the ROS level to nearly the same level as in as the control. Additionally, PQ can destroy the antioxidant system and cause oxidative damage. LDH is related to cell viability and membrane integrity, and MDA can be used to evaluate oxidative stress as an indicator of membrane lipid peroxidation [34,35]. Our results showed that An can prevent LDH leakage and reduce MDA activity. The antioxidant defense systems include enzymatic and non-enzymatic antioxidant mechanisms. As a main antioxidant enzyme, SOD exerts a protective effect against oxidative stress-induced injury [36]. GPx is a non-enzymatic antioxidant that may be associated with organic antioxidation [37].

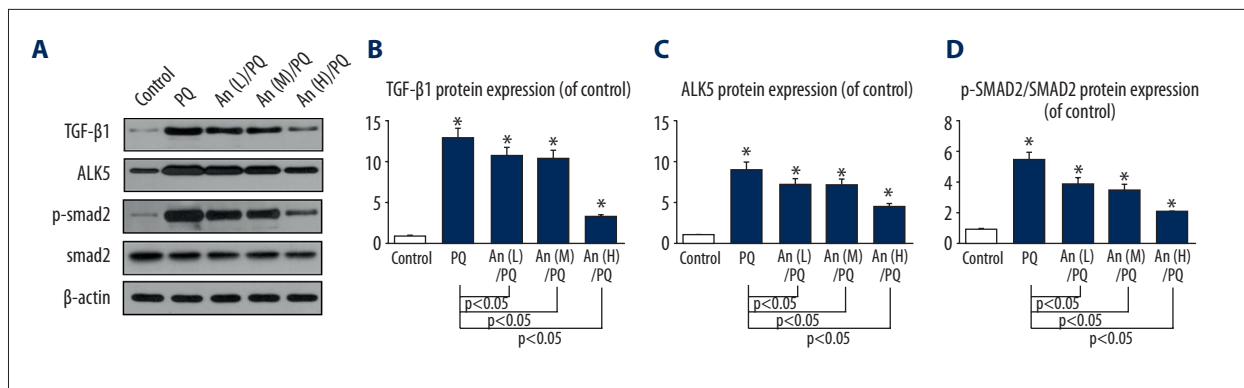


Figure 5. An suppressed the expressions of TGF-β1 and ALK5 and the ratio of p-smad/smad. **(A)** The protein levels of TGF-β1, ALK5, p-smad, and smad as shown by Western blot analysis. The protein levels of **(B)** TGF-β1 and **(C)** ALK5 were decreased by An and **(D)** the ratio of p-smad/smad was also reduced by An. * $P < 0.05$ compared with control group.

In our study, the levels of SOD and GPx were obviously improved by An. These results suggest that An can alleviate PQ-induced oxidative damage.

In the EMT process, epithelial cells lose epithelial markers (E-cadherin) and acquire mesenchymal markers (vimentin), accompanied by obliterated cell–cell adhesion and improved motility [38]. α -SMA is reported to be a specific protein of myofibroblast differentiation, and col-I is highly expressed in fibrotic lung tissues [39,40]. We found that PQ enhanced the expression of E-cad, and the levels of α -SMA, vimentin, and col-I were decreased by PQ, suggesting that PQ can induce EMT and lead to increased EMT events in RLE-6TN cells. However, An can reverse the expressions of these molecules.

As a major inducement of EMT [41], TGF-β1 can bind and activate ALK5, and the activated ALK5 can phosphorylate Smad2 and Smad3 [42] to form heteromeric complexes with Smad4, which translocate into the nucleus, leading to EMT [43]. However, EMT has been reported to be related to smad2 signaling in multiple cancer cell types [44,45]. Meanwhile, it was revealed that TGF-β1 can trigger EMT in lung cancer cells [46].

References:

- Dinis-Oliveira RJ, Duarte JA, Sánchez-Navarro A et al: Paraquat poisonings: Mechanisms of lung toxicity, clinical features, and treatment. *Crit Rev Toxicol*, 2008; 38(1): 13–71
- Suntres ZE: Role of antioxidants in paraquat toxicity. *Toxicology*, 2002; 180(1): 65–77
- Buckley IBG, Nicholas A: Medical management of paraquat ingestion. *Br J Clin Pharmacol*, 2011; 72(5): 745–57
- Li LR, Sydenham E, Chaudhary B, You C: Glucocorticoid with cyclophosphamide for paraquat-induced lung fibrosis. *Cochrane Database Syst Rev*, 2014; (8): CD008084
- Yeo CD, Kim JW, Kim YO et al: The role of pentraxin-3 as a prognostic biomarker in paraquat poisoning. *Toxicol Lett*, 2012; 212(2): 157–60
- Wang J, Zhu Y, Tan J et al: Lysyl oxidase promotes epithelial-to-mesenchymal transition during paraquat-induced pulmonary fibrosis. *Mol Biosyst*, 2015; 12(2): 499–507
- Lamouille S, Xu J, Derynck R: Molecular mechanisms of epithelial-mesenchymal transition. *Nat Rev Mol Cell Biol*, 2014; 15(3): 178–96
- Chapman HA: Epithelial-mesenchymal interactions in pulmonary fibrosis. *Ann Rev Physiol*, 2011; 73(1): 413–35
- Kage H, Borok Z: EMT and interstitial lung disease: A mysterious relationship. *Curr Opin Pulm Med*, 2012; 18(5): 517–23
- Bonnebarkay D, Reaney SH, Langston WJ, Di MD: Redox cycling of the herbicide paraquat in microglial cultures. *Brain Res Mol Brain Res*, 2005; 134(1): 52–56
- Castello PR, Drechsel DA, Patel M: Mitochondria are a major source of paraquat-induced reactive oxygen species production in the brain. *J Biol Chem*, 2007; 282(19): 14186–93
- Hung DZ: Paraquat induces lung alveolar epithelial cell apoptosis via Nrf-2-regulated mitochondrial dysfunction and ER stress. *Arch Toxicol*, 2012; 86(10): 1547–58

In the present study, TGF-β1 and ALK5 levels were significantly increased by PQ, suggesting that PQ induces TGF-β1 and ALK5 in RLE-6TN cells. An attenuated the expressions of the TGF-β1 and ALK5. Meanwhile, the ratio of p-smad2/smad2 induced by PQ was markedly decreased by An. These results suggest that An can inhibit PQ-induced EMT by regulating TGF-β1, ALK5, and smad2 in RLE-6TN cells.

Conclusions

We demonstrated that anthocyanin can attenuate PQ-induced apoptosis and EMT in RLE-6TN cells. Furthermore, anthocyanin can suppress the expression of TGF-β1, reduce the level of ALK5, and inhibit the phosphorylation of smad2. These results are the first to show the effect of anthocyanin in the treatment of PQ-induced lung injury.

Conflict of interest

None.

13. Dinis-Oliveira RJ, Sousa C, Remião F et al: Sodium salicylate prevents paraquat-induced apoptosis in the rat lung. *Free Radic Biol Med*, 2007; 43(1): 48–61
14. Takeyama N, Tanaka T, Yabuki T, Nakatani T: The involvement of p53 in paraquat-induced apoptosis in human lung epithelial-like cells. *Int J Toxicol*, 2004; 23(1): 33–40
15. Chen J, Zeng T, Bi Y et al: Docosahexaenoic acid (DHA) attenuated paraquat induced lung damage in mice. *Inhal Toxicol*, 2013; 25(1): 9–16
16. Chen Y, Nie YC, Luo YL et al: Protective effects of naringin against paraquat-induced acute lung injury and pulmonary fibrosis in mice. *Food Chem Toxicol*, 2013; 58(4): 133–40
17. He X, Wang L, Szklarz G et al: Resveratrol inhibits paraquat-induced oxidative stress and fibrogenic response by activating the nuclear factor erythroid 2-related factor 2 pathway. *J Pharmacol Exp Ther*, 2012; 342(1): 81–90
18. Santos RS, Silva PL, Oliveira GP et al: Effects of oleonic acid on pulmonary morphofunctional and biochemical variables in experimental acute lung injury. *Respir Physiol Neurobiol*, 2011; 179(2–3): 129–36
19. Huang W-D, Wang J-Z, Lu Y-Q et al: Lysine acetylsalicylate ameliorates lung injury in rats acutely exposed to paraquat. *Chin Med J (Engl)*, 2011; 124(16): 2496–501
20. Takikawa M, Inoue S, Horio F, Tsuda T: Dietary anthocyanin-rich bilberry extract ameliorates hyperglycemia and insulin sensitivity via activation of AMP-activated protein kinase in diabetic mice. *J Nutr*, 2010; 140(3): 527–33
21. Kang MK, Li J, Kim JL et al: Purple corn anthocyanins inhibit diabetes-associated glomerular monocyte activation and macrophage infiltration. *Am J Physiol Renal Physiol*, 2012; 303(7): F1060–69
22. Khan MS, Ali T, Kim MW et al: Anthocyanins protect against LPS-induced oxidative stress-mediated neuroinflammation and neurodegeneration in the adult mouse cortex. *Neurochem Int*, 2016; 100: 1–10
23. Wei J, Wu H, Zhang H et al: Anthocyanins inhibit high glucose-induced renal tubular cell apoptosis caused by oxidative stress in db/db mice. *Int J Mol Med*, 2018; 41(3): 1608–18
24. Jiang ZH, Chen C, Li XS et al: Anthocyanin attenuates alcohol-induced hepatic injury by inhibiting oxidative stress and proinflammation signaling. *Planta Med*, 2014; 80(16): P2B86
25. Hariri BM, Payne SJ, Bei C et al: In vitro effects of anthocyanidins on sinonasal epithelial nitric oxide production and bacterial physiology. *Am J Rhinol Allergy*, 2016; 30(4): 261–68
26. Ouanouki A, Lamy S, Annabi B: Anthocyanidins inhibit epithelial-mesenchymal transition through a TGFβ/Smad2 signaling pathway in glioblastoma cells. *Mol Carcinog*, 2016; 56(3): 1088–99
27. Yong Z, Wang J, Meng X et al: A positive feedback loop promotes HIF-1α stability through miR-210-mediated suppression of RUNX3 in paraquat-induced EMT. *J Cell Mol Med*, 2017; 21(12): 3529–39
28. Osorio F, Lambrecht B, Janssens S: The UPR and lung disease. *Semin Immunopathol*, 2013; 35(3): 293–306
29. Toygar M, Aydin I, Agilli M et al: The relation between oxidative stress, inflammation, and neopterin in the paraquat-induced lung toxicity. *Hum Exp Toxicol*, 2015; 34(2): 198–204
30. Ren M, Wang YM, Zhao J et al: Metallothioneins attenuate paraquat-induced acute lung injury in mice through the mechanisms of anti-oxidation and anti-apoptosis. *Food Chem Toxicol*, 2014; 73(73): 140–47
31. Omura T, Asari M, Yamamoto J et al: Sodium tauroursodeoxycholate prevents paraquat-induced cell death by suppressing endoplasmic reticulum stress responses in human lung epithelial A549 cells. *Biochem Biophys Res Commun*, 2013; 432(4): 689–94
32. Yang W, Tiffany-Castiglioni E, Koh HC, Son IH: Paraquat activates the IRE1/ASK1/JNK cascade associated with apoptosis in human neuroblastoma SH-SY5Y cells. *Toxicol Lett*, 2009; 191(2–3): 203–10
33. Zhang J, He Z, Guo J et al: Sulfiredoxin-1 protects against simulated ischemia/reperfusion injury in cardiomyocyte by inhibiting PI3K/AKT-regulated mitochondrial apoptotic pathways. *Biosci Rep*, 2016; 36(2): pii: e00325
34. Yang X, Wang Q, Wang C et al: Synthesis and protective effects of Kaempferol-3'-sulfonate on hydrogen peroxide-induced injury in vascular smooth muscle cells. *Chem Biol Drug Des*, 2016; 87(6): 841–48
35. Cai Y, Hu X, Yi B et al: Glucagon-like peptide-1 receptor agonist protects against hyperglycemia-induced cardiocytes injury by inhibiting high mobility group box 1 expression. *Mol Biol Rep*, 2012; 39(12): 10705–11
36. Iacobazzi D, Mangialardi G, Gubernator M et al: Increased antioxidant defense mechanism in human adventitia-derived progenitor cells is associated with therapeutic benefit in ischemia. *Antioxid Redox Signal*, 2014; 21(11): 1591–604
37. Marcil V, Lavoie JC, Emonnot L et al: Analysis of the effects of iron and vitamin C co-supplementation on oxidative damage, antioxidant response and inflammation in THP-1 macrophages. *Clin Biochem*, 2011; 44(10–11): 873–83
38. Tiwari N, Ghelof A, Tatari M, Christofori G: EMT as the ultimate survival mechanism of cancer cells. *Semin Cancer Biol*, 2012; 22(3): 194–207
39. Hu M, Che P, Han X et al: Therapeutic targeting of SRC kinase in myofibroblast differentiation and pulmonary fibrosis. *J Pharmacol Exp Therap*, 2014; 351(1): 87–95
40. Huang M, Wang YP, Zhu LQ et al: MAPK pathway mediates epithelial-mesenchymal transition induced by paraquat in alveolar epithelial cells. *Environ Toxicol*, 2016; 31(11): 1407–14
41. Chen HN, Yuan K, Xie N et al: PDLIM1 stabilizes the E-cadherin/β-catenin complex to prevent epithelial-mesenchymal transition and metastatic potential of colorectal cancer cells. *Cancer Res*, 2016; 76(5): 1122–34
42. Medina C, Santos-Martinez MJ, Santana A et al: Transforming growth factor-beta type 1 receptor (ALK5) and Smad proteins mediate TIMP-1 and collagen synthesis in experimental intestinal fibrosis. *J Pathol*, 2011; 224(4): 461–72
43. Shi S, Zhao J, Wang J et al: HPIP silencing inhibits TGF-β1-induced EMT in lung cancer cells. *Int J Mol Med*, 2017; 39(2): 479–83
44. Oft M, Akhurst RJ, Balmain A: Metastasis is driven by sequential elevation of H-ras and Smad2 levels. *Nat Cell Biol*, 2002; 4(7): 487–94
45. Lv ZD, Kong B, Li JG et al: Transforming growth factor-beta 1 enhances the invasiveness of breast cancer cells by inducing a Smad2-dependent epithelial-to-mesenchymal transition. *Oncol Rep*, 2013; 29(1): 219–25
46. Willis BC, Borok Z: TGF-β-induced EMT: Mechanisms and implications for fibrotic lung disease. *Am J Physiol*, 2007; 293(3): 525–34